Analysis of pluviometric data collected in the Apennine environment through traditional sensors and laser disdrometer

Author: Clizia Annella[1,2], clizia.annella@studenti.unisalento.it

Supervisor: Vincenzo Capozzi[1]

[1] Università degli studi di Napoli "Parthenope", [2] Università del Salento

Abstract

A detailed knowledge on rainfall properties is important in many fields and applications, such as soil erosion, agriculture, pollution wash-off in urban environments and road conditions. Surface precipitation measures are traditionally handled by tipping bucket or weighing gauges. An appealing alternative is offered by optical laser disdrometers, which are able to estimate not only the rainfall amount and intensity, but also the number, the size and the velocity of droplets. However, disdrometric measurements are subjected to different sources of errors, especially in strong rain and/or strong wind conditions; therefore, it is recommended to compare the data with those obtained with a conventional rain gauge in order to ensure accurate measurement. In this paper, a Thies Clima laser disdrometer is compared with a tipping bucket rain gauge (sensor FAK010AA) in terms of 10-minutes average rainfall rate and total rainfall accumulation at an apenninic site in southern Italy (Montevergine, 1280 m slm). The performance of Thies disdrometer are evaluated with respect to 35 rainfall events using some common statistical indicators. In the attempt to minimize sampling errors, a filtering process on disdrometer data is introduced: the filtering improves the agreement between data detected by the rain gauge and the disdrometer by 10% and stabilizes the rainfall estimation from disdrometer by reducing the standard deviation of the indicators. However, the disdrometer tends to almost systematically underestimate cumulative rainfall (by 8% considering all analyzed events). Wind effects on disdrometer spectrographs collected at 1-min time resolution are also investigated: for wind speed exceeding 1.5 m s^{-1}, more than half of detected combinations of velocity-diameter classes differ more than 50% with the theoretical fall velocity for rain events.

Keywords: optical disdrometer, drop size distribution, fall velocity, velocity–diameter relationship

1. Introduction

Detailed knowledge on rainfall amount and its characteristics is useful in a lot of different applications and fields. As an example, Toivonen and Kantonen (2001) investigated the impact of weather conditions on winter road traffic and the importance to provide information about the type of particles to reduce the risk of an accident. Other applications concern the study of a relationship between soil erosion and rainfall characteristics (Cruse et al. 2006) and the aerosol-precipitation interaction (Castro et al. 2010). Nowadays, many raindrop measurement techniques are available; initial manual methods, such as stain method, flour pellet method, oil immersion and photographic methods, recently evolved in automated devices such as disdrometers. The latter are weather sensors able to estimate the number, the size and the velocity of precipitation particles. Due to their affordable costs, low power consumption and maintenance requirements, such devices are more and more employed in both operational and research contexts. In last years, disdrometers have been used for many hydrometeorological tasks, as well as for the evaluation of hydrometeors classification algorithms developed from dual-polarization weather radar measurements (Pickering at al. 2019).

The accuracy of such instruments may be influenced by several factors, such as wind and turbulence conditions, which may modify the angle of fall direction and therefore introduce an error in the velocity measurements of particles (Kathiravelu et al. 2016). Measurement inaccuracy is also related to an

overestimation of particle size for simultaneous drops, which are detected as one. Another erroneous classification concerns the margin fallers, i.e. drops that fall at the edge of sensors sampling area, which results in an underestimation of droplets size. A solution to mitigate this problem consists in adopting a modified sampling area according to the particle size (Angulo Martinez et al. 2018). Droplets may also be intercepted by the external structure of disdrometer and eventually break and splash away in smaller but accelerated drops. These effects may increase during intense events and modify the drop-size distribution spectra. Due to measurements errors just mentioned, a comparison between data obtained from disdrometer and a traditional rain gauge is recommended in order to assess the accuracy of rain intensity and amount measurements.

Many studies compare different types of disdrometers and investigate the estimated precipitation parameters, whose differences can be explained by the different design and internal data processing of devices (e.g. Johannsen et al. 2020; Gires et al. 2018; Adirosi et al. 2018). However, there are only few studies focused on the assessment of disdrometer performance with respect to reference traditional gauges (e.g. Lanza and Vuerich 2012; Lanzinger et al. 2006; Fehlmann et al. 2020). This work proposes a contribute to this research path, by investigating the performance of the optical laser disdrometer produced by Thies Clima, a well-known device which allows a near-continuous (1-min resolution time) monitoring of precipitation intensity a type.

Using a dataset collected between December 2019 and September 2020 in a mountainous site of Southern Italy (Montevergine Observatory, LAT = 40.936502, LON = 14.72915, 1280 m asl), the performance of Thies disdrometer have been analyzed and discussed in terms of two essential precipitation parameters: the rainfall intensity (mm h^{-1}) and the rainfall amount (mm). The benchmark used as reference is a tipping bucket rain gauge, the FAK010AA of MTX srl, a collector with a calibrated circular area of 400 cm^2 whose technical specifications meets the World Meteorological Organization (WMO) recommendations. The disdrometer and rain-gauge data have been compared on 10-min basis using some familiar statistical scores (such as BIAS and RMSE) for quantitative evaluations. In this research, some efforts have been also devoted to the analysis of wind effect on disdrometer velocity-diameter spectrograph, an aspect scarcely considered in literature (Friedrich et al. 2013; Capozzi et al. 2020), but that is able to produce unrealistic artifacts.

The paper is organized as follows. Section II describes data and methods, focusing on devices characteristics and principles of functioning, dataset description and disdrometric data processing. Moreover, this section provides details about the criteria used to compare the data collected by the instruments. Section III discusses the results, whereas in Section IV the conclusions are drawn.

2. Data and methods

2.1. Brief description of devices functioning

The measurement devices involved in this work are the Thies Clima disdrometer and the FAK010AA rain gauge sensor. The Thies disdrometer is a laser optical device and provides information on precipitation drop spectra and hydrometeor type (drizzle, rain, snow, hail and mixed precipitation). A laser-optical beam source produces an infrared (780nm) parallel-beam and the optical intensity is transformed into an electrical signal by a photo diode placed on the receiver side (Thies Clima 2015). Thies working principle is light occlusion and when drops pass through the laser beam, the receiving signal is reduced according to the diameter of the hydrometeors. Velocity is determined from the duration of reduced signal, whilst the diameter is calculated from the obscuration amplitude. The sampling area is 45.6 cm^2, result of a 20 mm wide and 0.75 mm thick beam. The internal programming applies some correction in the rainfall measurement and particles are checked for plausibility, although the manual does not specify the details. Precipitation type is determined from the empirical relationship between fall velocity and drop diameter (Gunn and Kinzer 1949) and a further check on temperature is included to improve the classification: precipitations with a temperature of below -4°C are automatically classified as solid while those with a temperature of above 9°C are accepted as

liquid by default. Thies memorizes data over one minute and groups particles into 22 and 20 classes of diameter size and fall velocity ranging from 0.125 to 9 mm and from 0 to 12 ms^{-1}, respectively. In addition, rain rate, precipitation amount and precipitation type data computed from Thies software are also available.
The FAK010AA is a precipitation sensor with a collecting area of 1000 cm^2. The collector is made of anodized aluminium and the shape prevents rain from splashing in and out. An appropriate circular deflector reduces the undesired effects of the turbulence caused by wind. When the precipitation fills one of the collectors, the tipping bucket loses balance, overturns, and puts the empty bucket in the collection position. The instrument reports upon the event by generating an electrical output signal. The process then repeats itself. When the precipitation is solid (snow or hail), the measurement is carried out evaluating the amount of water released by the melting. This rain gauge has an accuracy of 2% over the entire operating range (0-300 mm h^{-1}) and a resolution of 0.2 mm.

2.2. Measurement period and location

The considered dataset includes rainy events occurred between December 2019 and September 2020 in the experimental site of Montevergine observatory. The latter is located in Southern Apennines near the top of the Partenio mountains (Fig. 1a) and was established in 1884 (Capozzi et al. 2020). The meteorological instruments, an automatic weather station (AWS), the FAK010AA rain gauge and the Thies disdrometer are placed on the observatory terrace (Fig. 1b).

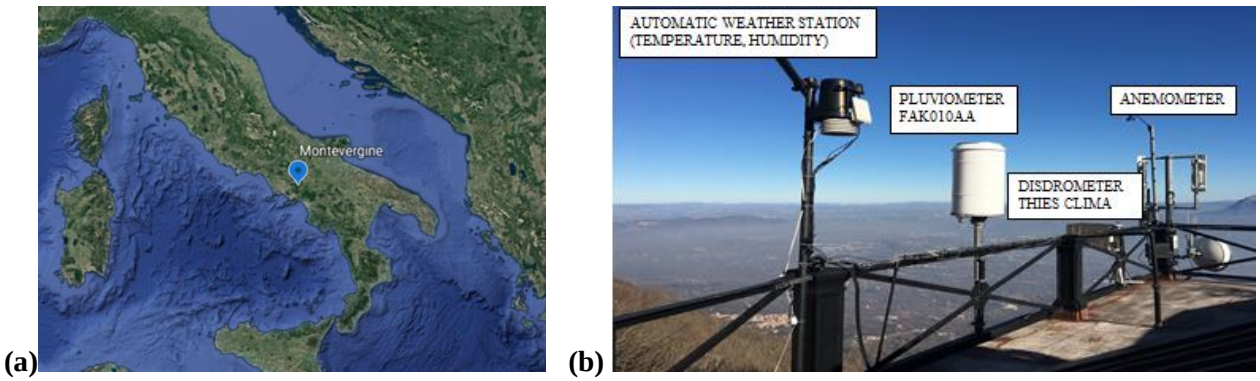

Fig. 1 (a) Map of Italy showing the location of Montevergine Observatory, LAT = 40.936502, LON = 14.72915, 1280 m asl. (b) The measurement devices placed on the observatory terrace: automatic weather station (temperature and humidity), FAK010AA rain gauge , Thies disdrometer and three-cup anemometer.

Among all available events, some have been discarded due to the very strong winds accompanying the precipitation and to the presence of solid hydrometeors (graupel, snow and hail). The resulting dataset consists of 35 rainfall events and encompasses a wide spectrum of meteorological scenarios, including different precipitation regimes (convective, stratiform and orographic) as well as different synoptic and mesoscale forcing. Table 1 provides a list of the events, including total precipitation amount and average rainfall rate recorded by FAK010AA rain gauge, as well as average wind speed measured by AWS. The average rain rate varies between 1.2 mm h^{-1} (lower limit detected by rain gauge) and 10.5 mm h^{-1}, whilst cumulative rainfall ranges between 1 mm and 124 mm. For each event, disdrometric data, i.e. the number of hydrometeors collected for each class of velocity and diameter, are available with a resolution of 1 minute. Other useful meteorological data, collected by AWS, such as air temperature, relative humidity, atmospheric pressure, wind speed (average and gust) and wind direction are still available with the same temporal resolution. The FAK010AA rain gauge data, i.e. rainfall amount and average rainfall intensity, are also stored with a 1-minutes temporal resolution.

DATE (dd/mm/yy)	ID NUMBER	AVERAGE RAIN RATE (mm h^{-1})	TOTAL PRECIPITATION AMOUNT (mm)	AVERAGE WIND SPEED (m s^{-1})
9/12/2019	1	4.3	16.7	1.7
20/12/2019	2	2.5	8.3	2.2
25/1/2020	3	1.4	1.8	0.9
26/1/2020	4	1.7	5.0	0.4
27/1/2020	5	2.1	1.4	2.7
29/1/2020	6	1.8	6.8	1.9
10/2/2020	7	1.7	4.0	0.9
11/2/2020	8	1.2	1.0	2.2
14/2/2020	9	4.5	19.6	1.4
28/2/2020	10	3.9	25.0	2.3
1/3/2020	11	4.5	8.2	2.2
2/3/2020	12	2.6	8.8	3.5
27/3/2020	13	2.0	10.2	1.8
20/4/2020	14	2.0	28.4	1.4
22/4/2020	15	3.0	29.6	4.5
23/4/2020	16	1.2	2.2	8.0
28/4/2020	17	1.8	1.2	1.6
29/4/2020	18	3.6	1.2	0.7
3/5/2020	19	10.2	27.2	3.3
20/5/2020	20	1.9	8.6	3.4
29/5/2020	21	10.0	10.0	1.3
30/5/2020	22	1.8	7.0	3.5
31/5/2020	23	4.4	7.6	1.3
1/6/2020	24	1.6	1.0	0.7
3/6/2020	25	6.9	4.6	5.9
5/6/2020	26	3.3	28.2	2.6
8/6/2020	27	5.7	4.2	1.6
10/6/2020	28	6.2	10.4	4.7
11/6/2020	29	2.0	5.4	2.3
16/6/2020	30	2.1	5.0	4.0
21/6/2020	31	5.1	11.8	2.3
4/7/2020	32	2.6	2.6	2.8
17/7/2020	33	2.3	7.0	2.5
18/7/2020	34	5.4	3.6	1.9
27/9/2020	35	10.5	124.4	2.9

Table 1 List of the selected events including average rain rate recorded and total precipitation amount (mm) by FAK010AA rain gauge (mm h^{-1}), as well as average wind speed measured by AWS (m s^{-1}).

2.3.Process of data filtering

An “ad-hoc” filtering procedure has been applied to raw disdrometric data in order to remove spurious measurements due to wind, margin faller and splashing effects. The disdrometer provides a matrix counting the number of particles with a given size and fall velocity recorded at 1-min intervals. The filtering process

consists in three steps. First, for each instant (one minute), particles with fall velocity greater or equal to 9.5 m s^{-1} and diameter smaller or equal to 1.875 mm are deleted and if the number of recorded classes is smaller than three, precipitations are considered null. The second step consists in a weighted power fit of data, where weights are obtained as follows:

$$w_{ijk} = \frac{a_{ijk}}{ms_k} \tag{1}$$

where a_{ijk} is the number of particles with fall velocity i and diameter j and ms_k is the absolute maximum value in a given k- time instant. Hydrometeors classes differing more than 60% with the power fit are discarded. In the last step, the fitting procedure is repeated without weights and classes that are within ±80% with power fit are accepted. As a result, a filtered version of the original disdrometric dataset has been obtained. A nice example of data filtering process is shown in Fig. 2, which allows to compare the empirical drop size-velocity relationship obtained through the procedure just described and that proposed by literature for rainy events (Atlas and Ulbrich, 1973). Filtering process applied to disdrometer raw data partially excludes the erroneously classified particles, as showed in Fig. 2b. Measurement inaccuracy may occur due to wind, simultaneous drops, margin fallers and splashing and may raise in heavy rainfall events. Fig. 3 presents a comparison between raw and filtered aggregated spectra for two events characterized by different average rain rate (1.1 mm h^{-1} and 9.7 mm h^{-1}, respectively) and average wind speed conditions (0.9 m s^{-1} and 3.3 m s^{-1}, respectively). It can be easily observed that the scenario with high rain rate and strong wind speed determines an increase of anomalous classes detected.

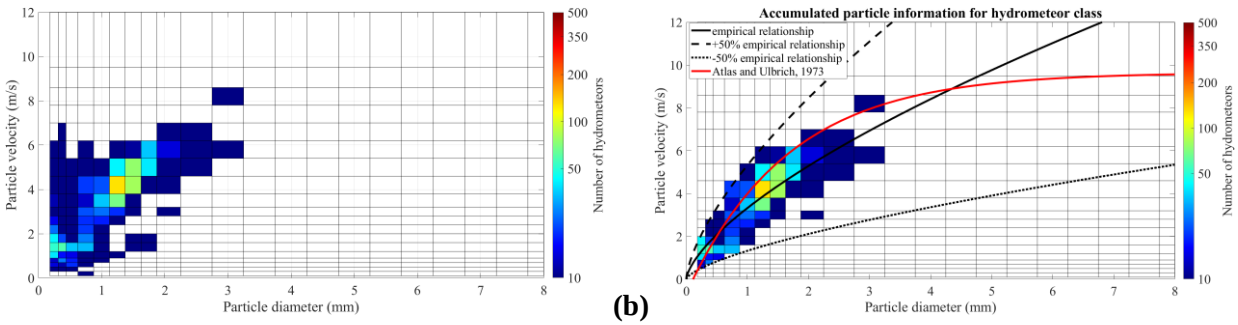

Fig. 2 Example of data filtering process showing a comparison of the empirical drop size-velocity relationship computed on raw (a) and filtered (b) disdrometric data and that proposed by literature for rainy events (Atlas and Ulbrich 1973). The color scale indicates the number of drops in each size-velocity class.

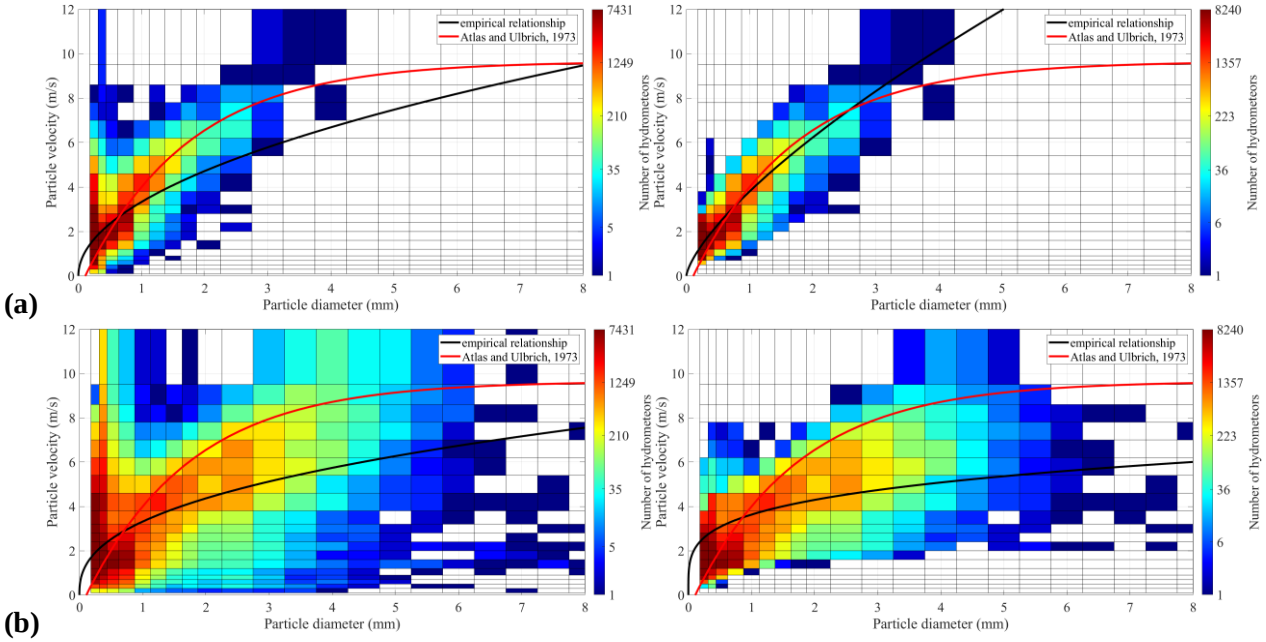

Fig. 3 Comparison between raw (left panel) and filtered (right panel) aggregated spectra measured by disdrometer for light (a) and high (b) rain rate events. The color scale indicates the number of drops in each size-velocity class.

2.4.Comparison of measurements and device performance

Since Thies Clima manufacturer does not report the exact equation used to calculate the precipitation amount and the rain rate, the latter have been derived from raw and filtered spectrographs by following equations (Angulo Martinez et al. 2018):

$$P = \frac{4\pi}{3} \sum_{i,j} \left(\frac{1}{A_j} N_{i,j} \left(\frac{D_j}{2} \right)^3 \right), \tag{2}$$

$$RR = \frac{P}{\Delta t}, \tag{3}$$

$$A_j = A \left(1 - \frac{D_j}{2w} \right), \tag{4}$$

Where P is the rainfall amount (mm), D_j is the diameter class j (mm), $N_{i,j}$ is the number of drops in size class j and velocity class i, RR is the rain rate (mmh^{-1}), A is sampling area of disdrometer (45.6 cm^2) and w is the width of laser beam (20 mm). The sampling area A is modified in A_j, according to the drop size, to avoid measurement issues related with margin fallers. To compare Thies disdrometer and gauge observations and bypass mismatches due to temporal shifts between measurements and due to different mean principle between two devices, both data have been aggregated on a 10-minutes period. The following statistical performance indicators have been used to quantify the difference between Thies Clima and FAK010AA rain gauge:

$$MAE = \frac{\sum_{i=1}^{n} |RR_{dis_i} - RR_{plu_i}|}{n} \tag{5}$$

$$BIAS = \frac{\sum_{i=1}^{n}(RR_{dis_i} - RR_{plu_i})}{n} \quad (6)$$

$$RMSEP = \sqrt[2]{\frac{\sum_{I=1}^{n}\left(\frac{RR_{dis_i} - RR_{plu_i}}{RR_{plu_i}}\right)^2}{n}} * 100\% \quad (7)$$

$$E = \frac{RR_{dis_i} - RR_{plu_i}}{RR_{plu_i}} * 100\% \quad (8)$$

$$RMSE = \sqrt[2]{\frac{\sum_{I=1}^{n}(RR_{dis_i} - RR_{plu_i})^2}{n}} \quad (9)$$

The comparison is made on records in which both instruments detect rain and the values of the rain gauge are taken as reference.

3. Results and discussion

For each of the selected rainy events, a systematic comparison between 10-min precipitation intensities and rainfall amount detected by FAK010AA rain gauge and Thies disdrometer has been performed. Fig. 4 sketches the cumulative precipitation sums of the raw (Fig. 4a) and filtered (Fig. 4b) disdrometer data as compared to the FAK010AA rain gauge. Full investigation period has been taken into account. A close inspection of this graph easily allows evaluating the benefits introduced by filtering process described in the previous section. The latter, in fact, improves the agreement between the two devices by 9% over the full period according to E, which is -7.7% for filtered data, +16.8% for raw data. Additional and relevant evidences are also provided by Fig. 5, which shows a scatter diagram between 10-min rainfall rate measurements collected by the two devices in the analysed period. The analysis of Fig. 5a, in which raw disdrometric data are shown, reveals important discrepancies between the two devices, especially for RR values greater than 20 mm h^{-1}. Such differences are well synthetized by RMSE value (1.96 mm h^{-1}) obtained from all considered events, as well as by its standard deviation (2.9 mm h^{-1}). Fig. 5b demonstrates that filtering procedure produces benefits on RMSE and its standard deviation, as well as on linear fit (blue line), which is closer to the reference line (highlighted in red). It is worth noting that the largest difference between the two instruments occur when rain rate is above 20 mm h^{-1}: in such circumstances, the filtered disdrometric data systematically underestimate the RR.

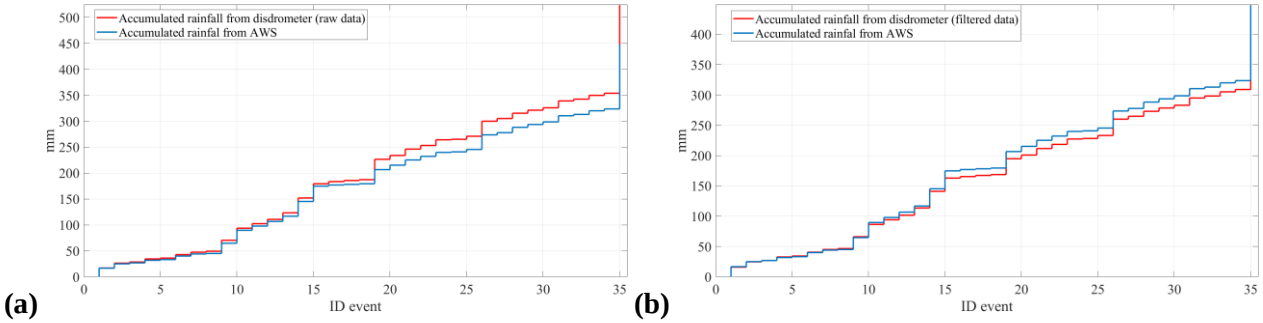

(a) **(b)**

Fig. 4 Comparison of 10-min cumulative precipitation sums (mm) between the raw (a) and filtered (b) disdrometer data and the FAK010AA rain gauge in full investigation period.

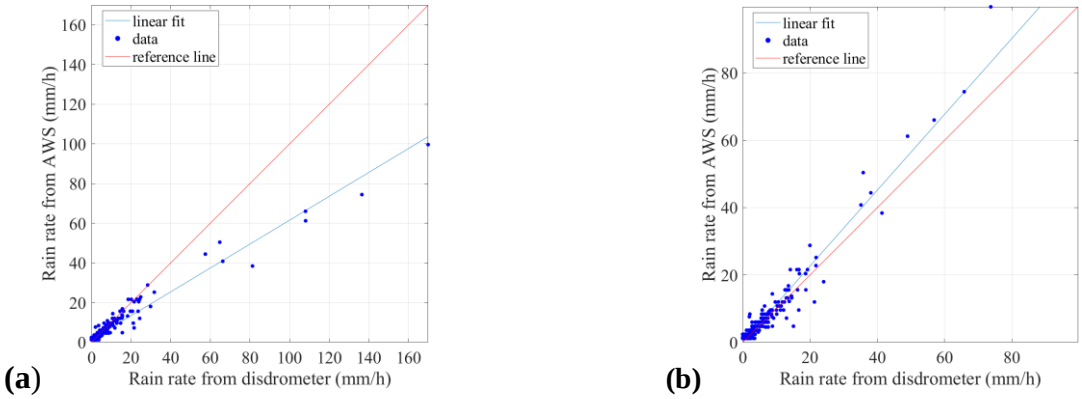

Fig. 5 Scatter diagram between 10-min RR measurements (mm h^{-1}) collected by Thies disdrometer (raw data (a) and filtered data (b)) and FAK010AA rain gauge in the analysed period. The linear fit is reported in both panels in order to highlight systematic errors and has respectively a slope of 0.6 (a) and 1.13 (b).

Fig. 6 presents MAE and BIAS value for each of the 35 rainy events, labelled on x-axis of both panel through their ID number (see Table 1). More specifically, red lines show the results obtained from raw Thies data, whereas blue line those achieved from filtered data. The impact of filtering process determines, for both scores, a reduction of standard deviation (Table 2). For MAE, whose optimal value is 1.0, a slight improvement can be also appreciated in terms of mean value, which reduces from 1.17 mm h^{-1} to 0.95 mm h^{-1}.

BIAS estimator gives a further and clear evidence of the change in the error "direction" from raw to filtered Thies data scenario. Looking at Fig. 6b, it is interesting highlighting that most relevant departures of BIAS scores from its optimal value (0.0) occurred for event #35 (27/09/2020), which is characterized by the highest average RR and P in the investigated time interval, and for event #28 (10/06/2020), in which both average RR and wind speed are relatively high. Thies disdrometer and FAK010AA have been also compared in terms of RMSEP; however, only a very slight improvement (from 48 to 47%) have been observed after filtering process.

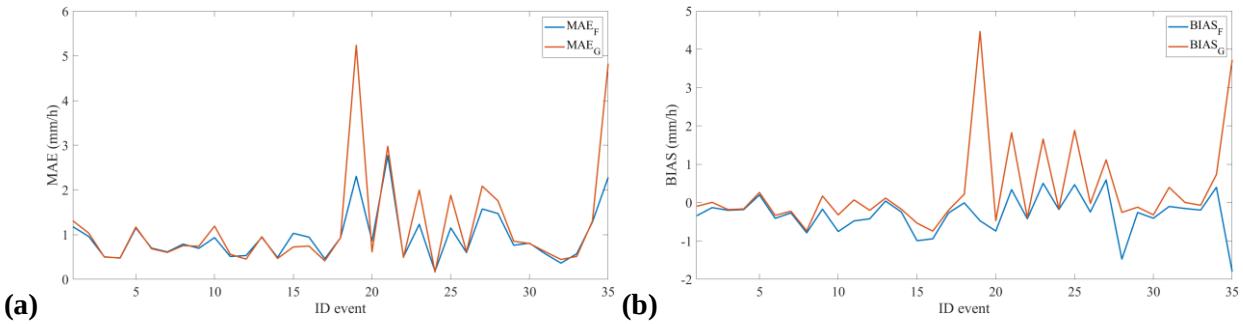

Fig. 6 MAE (a) and BIAS (b) value for each of the 35 rainy events. Red lines show the results obtained from raw Thies data (G), whilst blue lines from filtered data (F). Both indicators are in (mm h^{-1}).

	Raw data		Filtered data	
Statistical indicator	Mean (mm h^{-1})	Std (mm h^{-1})	Mean (mm h^{-1})	Std (mm h^{-1})
MAE	1.17	1.13	0.95	0.57
BIAS	0.3	1.14	-0.3	0.51
RMSE	1.96	2.9	1.29	0.98

Table 2 For each statistical indicator, mean and standard deviation are listed both for raw and filtered disdrometer data.

Finally, wind effects on raindrop size and velocity distribution recorded by disdrometer have been investigated. This analysis has been carried out using 1-min wind speed and raw disdrometric data. To avoid undesired temporal mismatching between Thies and AWS data, a careful manual inspection has been performed. The latter highlighted slight temporal misalignment between two devices in some events, which have been discarded for this analysis. Since disdrometric measurement errors increase with RR, in order to investigate wind influence, only light rain events, i.e. between 0.1 and 2.5 mm h^{-1}, have been considered. The approach used to evaluate the possible impact of wind on Thies velocity-diameter spectrograph starts from a classification of available data with respect to eight different wind speed thresholds (Table 3). The Thies spectrum collected in a determined time instant has been associated to a certain wind class if, in that instant, the average wind speed is within the limits of that class and if the wind gust meets the following criterion, defined as:

$$w_{max} \leq 0.5 * w_{tre_{up}} + w_{avg} \tag{10}$$

where w_{max} is the wind gust, w_{avg} is the average wind speed and $w_{tre_{up}}$ is the upper threshold of a determined wind class. Subsequently, the spectrographs associated to each wind classes have been aggregated through a simple sum of the hydrometeors detected for each velocity-diameter class. To quantify the number of drop-size classes erroneously categorized due to wind effects, for each wind group the ratio between the number of classes which differs by more than 50% with the Atlas and Ulbrich (1973) theoretical relationship and the total number of classes detected by the disdrometer has been computed. The actual number of droplets well classified has been determined as the ratio between the sum of particles inside the range $\mp$50% of the values imposed by the Atlas and Ulbrich (1973) relationship and the total number of hydrometeors detected by the disdrometer in each wind group. A graphical evidence of the results of this analysis is provided by Fig. 7. This figure presents the aggregated Thies spectrograph for different wind speed classes, ranging from calm wind (0-0.5 m s^{-1}) to moderate breeze winds (6-8 m s^{-1}). Combinations differing by more than 50% with the theoretical fall velocity are represented in the figure with a transparency. It can be easily noted that the number of anomalous velocity-diameter classes rapidly increase with increasing wind speed thresholds. From a quantitative point of view, the percentage of anomalous drop size classes goes from 43% in calm wind events to around 70% when wind speed is more than 8 m/s (Fig. 8a). Moreover, according to Fig. 8b, for wind speed ranging to 0 and 0.5 m s^{-1} almost the 70% of the hydrometeors is well classified. This percentage dramatically drops with increasing wind speed, reaching a value below 20% for wind speed exceeding 4 m s^{-1}.

Class	Lower threshold $w_{tre_{low}}$ (ms^{-1})	Upper threshold $w_{tre_{up}}$ (ms^{-1})
1	0	0.5
2	0.5	1.5
3	1.5	3
4	3	4
5	4	5
6	5	6
7	6	8
8	8	10

Table 3 Classification of available data with respect to eight different wind speed thresholds with $w_{avg} \in [w_{tre_{low}}, w_{tre_{up}})$.

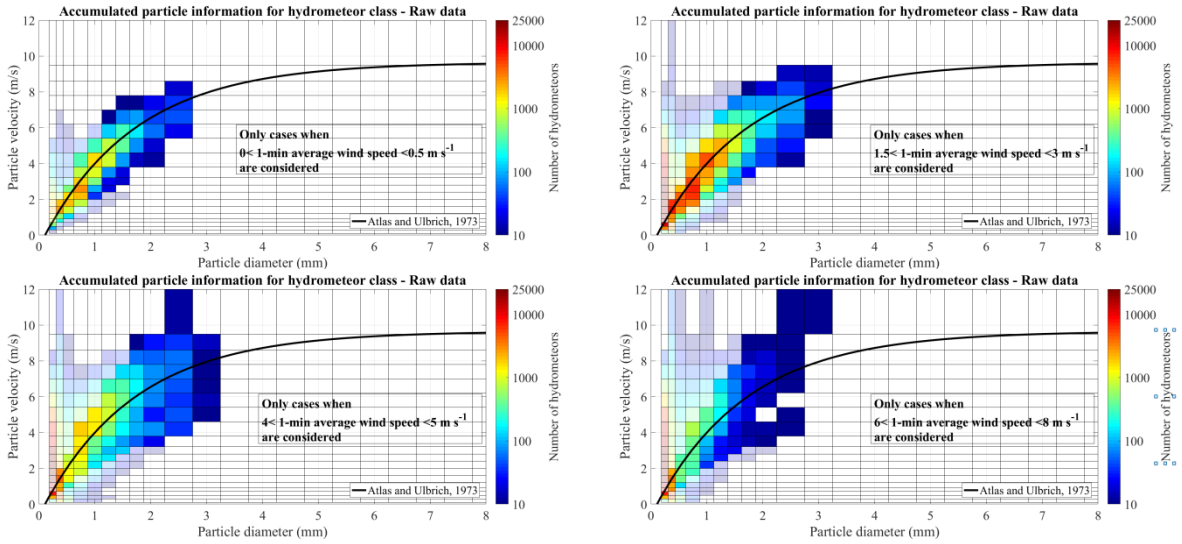

Fig. 7 Aggregated Thies spectrograph for different wind speed classes, ranging from calm wind (0-0.5 m s^{-1}) to moderate breeze winds (6-8 m s^{-1}). The color scale indicates the number of drops in each size-velocity class and deviation larger than 50% from theoretical drop size-velocity relationship are indicated in transparencies. Atlas and Ulbrich (1973) relationship is indicated as black line.

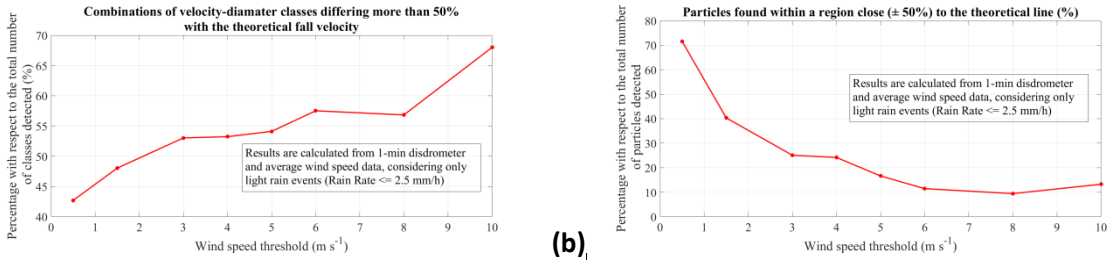

Fig. 8 Methods to quantify wind effect on Thies spectrograph. (a) Combinations of velocity-diameter classes differing more than 50% with the theoretical fall velocity (Atlas and Ulbrich 1973). (b) Particles found within a region close (±50%) to the theoretical line (Atlas and Ulbrich 1973).

4. Conclusions

In this work, the performance of a laser-optical disdrometer have been investigated in a well-instrumented apenninic site of Southern Italy. Using a dataset consisting of 35 rainy events occurred between December 2019 and September 2020, an extensive comparison between the disdrometer and a reference tipping bucket rain gauge (the FAK010AA) has been performed in terms of RR and P measures. The results have been discussed with the aid of some statistical scores, considering two different datasets of disdrometric measurements: a raw version, consisting of original data collected by device, and a filtered one. The latter has been obtained through an "ad-hoc" filtering procedure, which has been designed to remove spurious velocity-diameter classes.

All considered statistical scores have clearly highlighted the benefits introduced by the filtering procedure, which can be synthetized by the improvement observed in MAE (from 1.17 to 0.95 mm h^{-1}) , RMSE (from 1.96 to 1.29 mm h^{-1}) and E (from +16 to -8%). The agreement between Thies disdrometer and FAK010AA rain gauge is generally good, although the former almost systematically underestimated the rainfall amounts, especially when rain rate is above 20 mm h^{-1}. The last part of this research has been devoted to a focus on

wind speed impact on disdrometer spectrographs. This investigation reveals that for wind speed larger than 4 m s^{-1}, only about 20% of the detected hydrometeors belong to the theoretical velocity-diameter combinations for rain events.

Future research should be dedicated to the analysis of solid and mixed precipitation events, in order to assess the performance of Thies disdrometer in snow, graupel and hail conditions. Moreover, additional efforts should be carried out for a quantitative evaluation of wind impact on disdrometer RR and P measures.

References

Adirosi E, Roberto N, Montopoli M, Gorgucci E, and Baldini L (2018) Influence of disdrometer type on weather radar algorithms from measured DSD. Application to Italian climatology, Atmosphere 9:1–30. doi: 10.3390/atmos9090360

Angulo-Martínez M, Beguería S, Latorre, B and Fernández-Raga M (2018) Comparison of precipitation measurements by OTT Parsivel Parsivel^{2}and Thies LPM optical disdrometers. Hydrology and Earth System Sciences 22(5):2811–2837. doi:10.5194/hess-22-2811-2018

Atlas D, Ulbrich C W, Srivastava R C and Sekhon R S (1973) Doppler radar characteristics of precipitation at vertical incidence. Rev. Geophys. Space Phys. 11:1–35. doi:10.1029/RG011i001p00001

Capozzi V, Cotroneo Y, Castagno P, De Vivo C and Budillon G (2020) Rescue and quality control of sub-daily meteorological data collected at Montevergine Observatory (Southern Apennines). Earth System Science Data 12(2):1467-1487. doi: 10.5194/essd-12-1467-2020

Castro A, Alonso-Blanco E, González-Colino M, Calvo A I, Fernández-Raga M and Fraile R (2010) Aerosol size distribution in precipitation events in León, Spain. Atmos. Res. 96:421–435

Cruse R, Flanagan D, Frakenberger J, Gelder B, Herzmann D, James D, Krajewski W F, Kraszewski M, Laflen J, Opsomer J, and Todey D (2006) Daily estimates of rainfall, water runoff, and soil erosion in Iowa.J. Soil Water Conserv 61:191–199

Fehlmann M, Rohrer M, von Lerber A and Stoffel M (2020) Automated precipitation monitoring with the Thies disdrometer: biases and ways for improvement. Atmospheric Measurement Techniques 13(9): 4683-4698. doi: 10.5194/amt-13-4683-2020

Friedrich K, Higgins S, Masters F J and Lopez C R (2013) Articulating and stationary PARSIVEL disdrometer measurements in conditions with strong winds and heavy rainfall. J. Atmos. Ocean. Technol. 30:2063–2080. doi. 10.1175/JTECH-D-12-00254.1

Gires A, Tchiguirinskaia I, and Schertzer D (2018) Two months of disdrometer data in the Paris area. Earth Syst. Sci. Data 10:941–950. Doi: 10.5194/essd-10-941-2018

Gunn R and Kinzer G D (1949) The terminal velocity of fall for water droplets in stagnant air. Journal of Meteorology 6 (4): 243–248. doi:10.1175/1520-0469(1949)006<0243:TTVOFF>2.0.CO;2

Johannsen L L, Zambon N, Strauss P, Dostal T, Neumann M, Zumr D, Cochrane T A, Blöschl G and Klik A (2020) Comparison of three types of laser optical disdrometers under natural rainfall conditions. Hydrological Sciences Journal 65:4, 524-535. doi: 10.1080/02626667.2019.1709641

Kathiravelu G, Lucke T and Nicholas P (2016) Rain Drop Measurement Techniques. A Review, Water 8(1):29. doi. 10.3390/w8010029

Lanza L G and Vuerich E (2012) Non-parametric analysis of one-minute rain intensity measurements from the WMO Field Intercomparison. Atmos. Res. 103:52–59. doi: 10.1016/j.atmosres.2011.04.021

Lanzinger E, Theel M and Windolph H (2006) Rainfall amount and intensity measured by the Thies laser precipitation monitor, in:WMO Technical Conference on Meteorological and Environmental Instruments and Methods of Observation (TECO-2006), 4–6, Geneva, Switzerland

Pickering B S, Neely III R R and Harrison D (2019) The Disdrometer Verification Network (DiVeN): a UK network of laser precipitation instruments. Atmos. Meas. Tech 12: 5845–5861. doi: 10.5194/amt-12-5845-2019

Thies Clima (2015) Instruction for use. Laser precipitation monitor. Göttingen: Adolf Thies GmbH & Co. KG

Toivonen K and Kantonen J (2001) Road weather information system in Finland. Transportation Research Record: J. Transport. Res. Board 1741:21–25. doi:10.3141/1741-04